

## Use of multitracers for the study of water mixing in the Paraíba do Sul River estuary

Tháísa Abreu Souza<sup>a,\*</sup>, José Marcus Godoy<sup>a,b</sup>, Maria Luiza D.P. Godoy<sup>b</sup>, Isabel Moreira<sup>a</sup>, Zenildo L. Carvalho<sup>b</sup>, Marcos Sarmet M.B. Salomão<sup>c</sup>, Carlos E. Rezende<sup>c</sup>

<sup>a</sup>Departamento de Química, Pontifícia Universidade Católica, 22453-900 Rio de Janeiro, RJ, Brazil

<sup>b</sup>Instituto de Radioproteção e Dosimetria IRD/CNEN, 22780-160 Rio de Janeiro, RJ, Brazil

<sup>c</sup>Centro de Biotecnologia e Biotecnologia, Universidade Estadual do Norte Fluminense, 28013-600 Campos dos Goytacazes, RJ, Brazil

### ARTICLE INFO

#### Article history:

Received 27 March 2009

Received in revised form

8 July 2009

Accepted 9 November 2009

Available online 9 December 2009

#### Keywords:

Estuary

Multitracers

Radium isotopes

Silicon

Barium

Uranium

Salinity

Paraíba do Sul River

### ABSTRACT

Multitracers were used to study water mixing in the Paraíba do Sul River estuary region in August 2007 (dry season) and March 2008 (rainy season) and to evaluate the reach of the river plume in the direction of the open ocean. Two sampling campaigns were carried out, each in a different season. Based on these results, it was possible to conclude that the multitracers used in this study (salinity, Si, Ba and U, as well as the radium isotopes <sup>223</sup>Ra, <sup>224</sup>Ra, <sup>226</sup>Ra and <sup>228</sup>Ra) presented satisfactory results toward defining the plume reach and determining the residence time and water-mixing processes in the estuary. A strong correlation was observed between tracers and the distance to the coast. During the low river water discharge period, the riverine water took about 10 days to reach open ocean waters (salinity ~ 35). During the rainy period this value decreased to 6 days. Based on the radium results, it was possible to calculate diffusion coefficients ( $K_h$ ) of 23 km<sup>2</sup> d<sup>-1</sup> and 38 km<sup>2</sup> d<sup>-1</sup> for <sup>224</sup>Ra and <sup>223</sup>Ra, respectively, during the dry season (winter). Values of 65 km<sup>2</sup> d<sup>-1</sup> and 68 km<sup>2</sup> d<sup>-1</sup> for <sup>223</sup>Ra and <sup>224</sup>Ra, respectively, were found for the rainy period (summer).

© 2009 Elsevier Ltd. All rights reserved.

### 1. Introduction

Rivers represent a major pathway for the transportation of dissolved and particulate materials from continental to coastal regions, as well as to the oceans. During the transportation process, several factors (e.g., physical, chemical and biological) can modify the original geochemical forms and source signatures. Thus, the storage of organic and inorganic compounds, as well as their biogeochemical cycles, is strongly affected by different activities, including agriculture, urbanization and industrial development. Another important aspect of the global biogeochemical balance is related to load underestimation, which occurs when only large rivers are considered. Although medium and small catchments are generally disregarded, these systems can represent a large contribution for certain elements, especially in areas with intense human occupation.

Coastal waters present high concentrations of four dissolved radium isotopes (i.e., <sup>223</sup>Ra, <sup>224</sup>Ra, <sup>226</sup>Ra and <sup>228</sup>Ra), which come

from particle desorption processes and radium-enriched groundwater (Charette et al., 2008; McKee, 2008). In coastal environments, <sup>223</sup>Ra and <sup>224</sup>Ra (half-lives of 11.4 and 3.66 days, respectively) decay before reaching the continental shelf, whereas <sup>226</sup>Ra and <sup>228</sup>Ra (half-lives of 1600 and 5.7 years, respectively) concentrations should change only by mixing with lower activity seawater (Moore and Krest, 2004).

Several chemical, physical and biological processes are associated with the mixing of river and seawater in an estuary. The properties of water mixing in an estuary are controlled by ionic strength, pH, chemical composition, flocculation, removal of organisms and adsorption/desorption of constituents. All of these factors can strongly influence the flow of chemical species into the ocean (Lee et al., 2005).

The utility of one radioisotope as a tracer in marine systems depends on its chemical and radiochemical characteristics, as well as its origin and decay-time scale. All of the four radium isotopes can potentially be used as tracers. Because these isotopes behave conservatively, remaining in the water mass without precipitating, their apport levels are kept constant in the time necessary to develop a study to understand water-mixing processes. In the specific case of short half-life isotopes (<sup>223</sup>Ra and <sup>224</sup>Ra), the loss in

\* Corresponding author. Tel.: +55 (21) 35271802.

E-mail address: [abreu.thaísa@gmail.com](mailto:abreu.thaísa@gmail.com) (T.A. Souza).

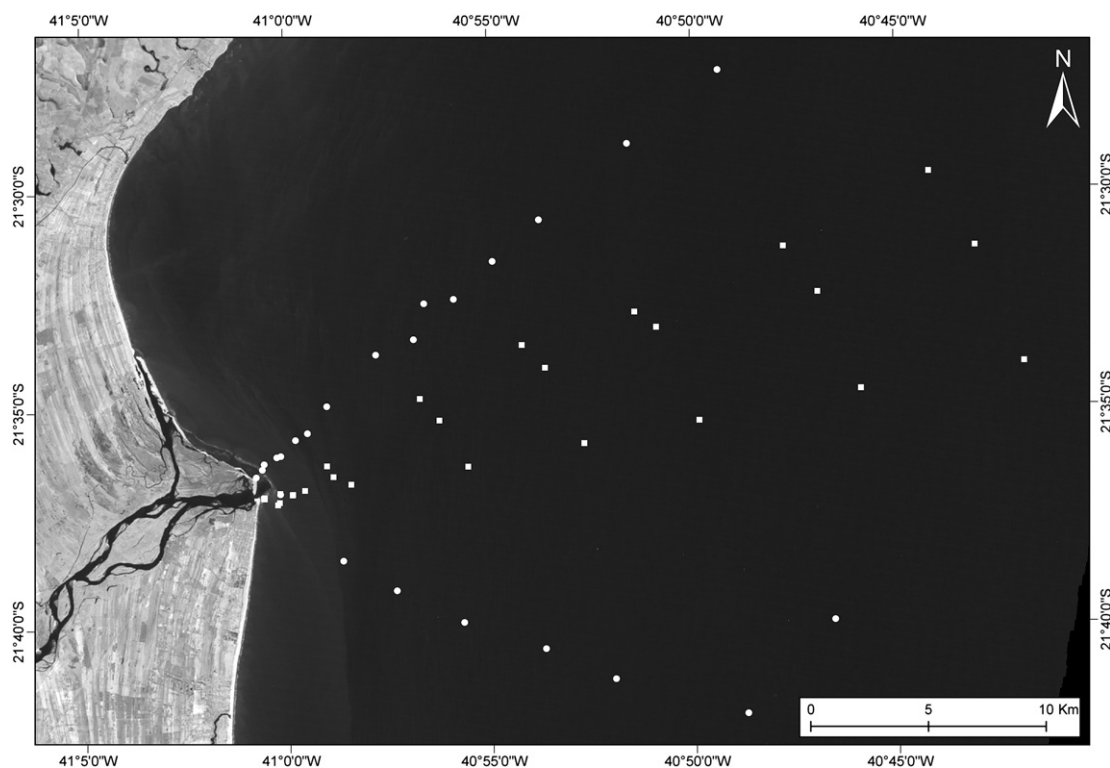


**Fig. 1.** Satellite imaging showing the study transects, chosen during the 1st and 2nd sampling periods. Legend: open dots correspond to the 1st sampling (August/2007) and the open squares to the 2nd sampling (March/2008).

occurrence levels owing to short-term decay is compensated by their continuous apportion into the water mass from sediments rich in thorium isotopes, promoting short-term quantitative regeneration.

The movement of dissolved elements in the water mass, tracers or not, is a function of the inherent processes in the natural movement of the water mass, including diffusion and advection. Evaluation of the activities of  $^{226}\text{Ra}$  and  $^{228}\text{Ra}$  serves to determine the relative importance of each process (Moore, 2000a,b). When the

distribution of these isotopes in the high-sea direction is predominated by a diffusive process, short half-life isotopes ( $^{223}\text{Ra}$  and  $^{224}\text{Ra}$ ) can be used to calculate  $K_h$  (diffusion coefficient) (Moore, 2000a,b). The product of  $^{228}\text{Th}$  decay,  $^{224}\text{Ra}$ , is an ideal tracer for marine processes that occur on a 1–10 day timescale. Processes with a timescale in this range include river-estuary and estuary-ocean exchanges, water mass movements on the continental platform, and interstitial water exchanges in salt marshes (Levy and Moore, 1985).

**Table 1**  
Results from Paraíba do Sul River transects (August 2007).

Sample	Distance (km)	Lat. (°S)	Long. (°W)	Salinity	(Bq m <sup>-3</sup> )				(nmol L <sup>-1</sup> )		(μmol L <sup>-1</sup> )	
					$^{223}\text{Ra}$	$^{224}\text{Ra}$	$^{226}\text{Ra}$	$^{228}\text{Ra}$	Ba	Si		
1	0.2	22°01'32"	41°01'33"	8.5	(0.285 ± 0.042)	(6.94 ± 0.57)	(1.12 ± 0.13) × 10 <sup>-3</sup>	(2.53 ± 0.28) × 10 <sup>-3</sup>	270	207		
2	0.8	21°60'43"	41°01'35"	18.9	(0.470 ± 0.050)	(12.7 ± 1.0)	(1.37 ± 0.15) × 10 <sup>-3</sup>	(3.33 ± 0.37) × 10 <sup>-3</sup>	204	143		
3	1.4	21°60'15"	41°00'48"	17.8	(0.331 ± 0.039)	(11.5 ± 1.0)	(8.57 ± 0.95) × 10 <sup>-4</sup>	(3.11 ± 0.35) × 10 <sup>-3</sup>	197	143		
4	2.5	21°59'51"	41°40'11"	26.6	(0.402 ± 0.037)	(11.26 ± 0.93)	(8.15 ± 0.91) × 10 <sup>-4</sup>	(4.21 ± 0.47) × 10 <sup>-3</sup>	131	71		
5	4.4	21°58'21"	41°38'38"	32.5	(0.193 ± 0.021)	(4.83 ± 0.42)	(7.41 ± 0.83) × 10 <sup>-4</sup>	(1.96 ± 0.22) × 10 <sup>-3</sup>	95	29		
6	7.4	21°56'27"	41°36'35"	33.4	(0.374 ± 0.032)	(6.33 ± 0.54)	(8.69 ± 0.97) × 10 <sup>-4</sup>	(3.32 ± 0.37) × 10 <sup>-3</sup>	80	20		
7	10.4	21°54'33"	41°34'36"	34.6	(0.246 ± 0.022)	(6.63 ± 0.60)	(7.25 ± 0.81) × 10 <sup>-4</sup>	(3.76 ± 0.42) × 10 <sup>-3</sup>	67	<14		
8	13.8	21°53'07"	41°31'53"	34.8	(0.243 ± 0.022)	(3.04 ± 0.26)	(1.04 ± 0.16) × 10 <sup>-3</sup>	(3.33 ± 0.38) × 10 <sup>-3</sup>	64	<14		
9	1.1	22°06'53"	41°17'59"	27.4	(0.53 ± 0.10)	(17.0 ± 1.5)	(3.47 ± 0.39) × 10 <sup>-4</sup>	(3.01 ± 0.34) × 10 <sup>-3</sup>	131	71		
10	4.9	22°10'06"	41°21'20"	31.7	(0.674 ± 0.070)	(15.5 ± 1.4)	(1.91 ± 0.21) × 10 <sup>-3</sup>	(2.98 ± 0.34) × 10 <sup>-3</sup>	95	34		
11	7.4	22°01'52"	41°00'28"	32.7	(0.506 ± 0.050)	(12.2 ± 1.1)	(1.12 ± 0.13) × 10 <sup>-3</sup>	(3.64 ± 0.41) × 10 <sup>-3</sup>	88	27		
12	10.5	22°04'11"	41°38'11"	35.0	(0.200 ± 0.026)	(4.15 ± 0.36)	(9.7 ± 1.1) × 10 <sup>-4</sup>	(4.35 ± 0.49) × 10 <sup>-3</sup>	73	<14		
13	14.1	22°05'26"	41°35'60"	35.5	(0.076 ± 0.012)	(2.34 ± 0.20)	(1.15 ± 0.13) × 10 <sup>-3</sup>	(3.35 ± 0.37) × 10 <sup>-3</sup>	65	<14		
14	17.3	22°06'46"	41°33'16"	35.7	(0.189 ± 0.021)	(2.35 ± 0.20)	(1.06 ± 0.12) × 10 <sup>-3</sup>	(3.77 ± 0.42) × 10 <sup>-3</sup>	63	<14		
15	22.9	22°07'53"	41°29'45"	35.7	(0.172 ± 0.018)	(1.96 ± 0.18)	(9.8 ± 1.1) × 10 <sup>-4</sup>	(3.78 ± 0.43) × 10 <sup>-3</sup>	64	<14		
16	25.2	22°09'12"	41°27'01"	35.7	(0.169 ± 0.020)	(1.74 ± 0.15)	(1.11 ± 0.12) × 10 <sup>-3</sup>	(3.23 ± 0.37) × 10 <sup>-3</sup>	61	<14		
17	0.7	21°60'57"	41°01'02"	30.7	(0.417 ± 0.045)	(12.1 ± 1.0)	(1.26 ± 0.14) × 10 <sup>-3</sup>	(3.40 ± 0.38) × 10 <sup>-3</sup>	109	43		
18	1.6	21°60'07"	41°00'26"	30.2	(0.344 ± 0.037)	(12.6 ± 1.1)	(1.01 ± 0.11) × 10 <sup>-3</sup>	(3.71 ± 0.42) × 10 <sup>-3</sup>	131	47		
19	3.1	21°59'21"	41°39'16"	32.1	(0.242 ± 0.029)	(13.4 ± 1.2)	(1.12 ± 0.13) × 10 <sup>-3</sup>	(3.90 ± 0.44) × 10 <sup>-3</sup>	109	43		
20	9.1	21°56'06"	41°35'16"	35.3	(0.241 ± 0.023)	(3.55 ± 0.31)	(1.39 ± 0.16) × 10 <sup>-3</sup>	(2.64 ± 0.30) × 10 <sup>-3</sup>	80	<14		
21	11.5	21°54'13"	41°33'10"	36.0	(0.235 ± 0.026)	(2.89 ± 0.22)	(1.24 ± 0.14) × 10 <sup>-3</sup>	(3.00 ± 0.34) × 10 <sup>-3</sup>	73	<14		
22	16.4	21°51'12"	41°29'58"	35.8	(0.198 ± 0.020)	(1.97 ± 0.15)	(1.61 ± 0.18) × 10 <sup>-3</sup>	(2.22 ± 0.26) × 10 <sup>-3</sup>	65	<14		
23	21.4	21°48'24"	41°26'35"	36.0	(0.157 ± 0.016)	(1.91 ± 0.16)	(1.66 ± 0.19) × 10 <sup>-3</sup>	(1.78 ± 0.21) × 10 <sup>-3</sup>	61	<14		
24	26.3	21°45'47"	41°22'19"	36.2	(0.127 ± 0.016)	(1.52 ± 0.12)	(1.77 ± 0.20) × 10 <sup>-3</sup>	(1.66 ± 0.19) × 10 <sup>-3</sup>	60	<14		

**Table 2**  
Results from Paraíba do Sul River transects (March 2008).

Sample	Distance (km)	Lat. (°S)	Long. (°W)	Salinity	(Bq m <sup>-3</sup> )				(nmol L <sup>-1</sup> ) (μmol L <sup>-1</sup> ) (nmol L <sup>-1</sup> )		
					<sup>223</sup> Ra	<sup>224</sup> Ra	<sup>226</sup> Ra	<sup>228</sup> Ra	Ba	Si	U
1	0.0	21°37'04"	41°00'56"	0.1	(0.106 ± 0.016)	(4.62 ± 0.39)	(9.0 ± 1.1) × 10 <sup>-4</sup>	(2.82 ± 0.32) × 10 <sup>-3</sup>	213	278	<0.84
2	0.6	21°37'10"	41°00'22"	13.9	(0.242 ± 0.030)	(9.80 ± 0.90)	(1.86 ± 0.21) × 10 <sup>-3</sup>	(2.71 ± 0.30) × 10 <sup>-3</sup>	185	158	3.46
3	1.2	21°36'58"	40°59'53"	15.9	(0.173 ± 0.019)	(7.06 ± 0.52)	(1.26 ± 0.14) × 10 <sup>-3</sup>	(2.50 ± 0.28) × 10 <sup>-3</sup>	172	149	4.41
4	3.2	21°36'19"	40°59'12"	10.6	(0.217 ± 0.017)	(6.29 ± 0.48)	(1.30 ± 0.15) × 10 <sup>-3</sup>	(2.55 ± 0.29) × 10 <sup>-3</sup>	199	173	1.76
5	8.2	21°31'49"	40°56'57"	18.4	(0.186 ± 0.018)	(5.67 ± 0.43)	(1.42 ± 0.16) × 10 <sup>-3</sup>	(3.11 ± 0.36) × 10 <sup>-3</sup>	158	126	5.34
6	13.2	21°33'32"	40°54'14"	22.3	(0.177 ± 0.022)	(4.07 ± 0.36)	(1.54 ± 0.17) × 10 <sup>-3</sup>	(1.27 ± 0.15) × 10 <sup>-3</sup>	47	47	<0.84
7	18.2	21°32'47"	40°51'28"	34.4	(0.135 ± 0.015)	(2.20 ± 0.16)	(1.74 ± 0.19) × 10 <sup>-3</sup>	(7.46 ± 0.86) × 10 <sup>-4</sup>	40	44	12.7
8	25.2	21°31'24"	40°47'57"	34.2	(0.118 ± 0.013)	(2.12 ± 0.16)	(1.53 ± 0.17) × 10 <sup>-3</sup>	(9.6 ± 1.1) × 10 <sup>-4</sup>	40	43	12.1
9	32.2	21°29'26"	40°44'18"	34.9	(0.069 ± 0.009)	(1.100 ± 0.095)	(1.27 ± 0.14) × 10 <sup>-3</sup>	(1.12 ± 0.13) × 10 <sup>-3</sup>	37	42	12.7
10	0.0	21°37'04"	41°00'56"	0.1	(0.178 ± 0.027)	(5.12 ± 0.40)	(1.53 ± 0.17) × 10 <sup>-3</sup>	(2.58 ± 0.29) × 10 <sup>-3</sup>	222	264	<0.84
11	0.6	21°37'10"	41°00'22"	22.6	(0.292 ± 0.028)	(9.66 ± 0.75)	(1.93 ± 0.22) × 10 <sup>-3</sup>	(2.21 ± 0.25) × 10 <sup>-3</sup>	128	112	6.85
12	1.6	21°36'32"	40°56'50"	1.0	(0.253 ± 0.024)	(8.66 ± 0.80)	(1.97 ± 0.22) × 10 <sup>-3</sup>	(3.63 ± 0.41) × 10 <sup>-3</sup>	238	233	<0.84
13	3.6	21°36'45"	40°56'30"	6.5	(0.146 ± 0.016)	(4.61 ± 0.35)	(1.03 ± 0.12) × 10 <sup>-3</sup>	(2.67 ± 0.30) × 10 <sup>-3</sup>	206	196	<0.84
14	8.6	21°35'15"	40°56'18"	13.4	(0.218 ± 0.026)	(6.83 ± 0.60)	(1.29 ± 0.14) × 10 <sup>-3</sup>	(2.85 ± 0.33) × 10 <sup>-3</sup>	181	151	2.96
15	13.6	21°33'58"	40°53'39"	34.4	(0.209 ± 0.020)	(4.06 ± 0.28)	(1.79 ± 0.20) × 10 <sup>-3</sup>	(1.58 ± 0.18) × 10 <sup>-3</sup>	45	48	12.2
16	18.6	21°31'06"	40°50'53"	33.9	(0.177 ± 0.018)	(2.66 ± 0.19)	(1.57 ± 0.18) × 10 <sup>-3</sup>	(1.10 ± 0.13) × 10 <sup>-3</sup>	42	45	11.9
17	25.6	21°32'18"	40°46'57"	34.4	(0.151 ± 0.017)	(2.12 ± 0.20)	(1.69 ± 0.19) × 10 <sup>-3</sup>	(1.12 ± 0.13) × 10 <sup>-3</sup>	39	43	12.3
18	32.6	21°31'24"	40°43'09"	34.7	(0.105 ± 0.017)	(1.37 ± 0.10)	(1.45 ± 0.16) × 10 <sup>-3</sup>	(9.6 ± 1.1) × 10 <sup>-4</sup>	41	42	12.0
19	0.0	21°37'04"	41°00'56"	0.1	(0.220 ± 0.029)	(7.15 ± 0.57)	(1.79 ± 0.20) × 10 <sup>-3</sup>	(2.90 ± 0.33) × 10 <sup>-3</sup>	241	339	<0.84
20	0.6	21°36'51"	41°00'22"	18.4	(0.419 ± 0.042)	(12.6 ± 1.2)	(2.14 ± 0.24) × 10 <sup>-3</sup>	(4.13 ± 0.47) × 10 <sup>-3</sup>	180	134	4.66
21	1.6	21°36'45"	40°59'32"	3.2	(0.166 ± 0.023)	(7.01 ± 0.56)	(1.55 ± 0.17) × 10 <sup>-3</sup>	(3.88 ± 0.44) × 10 <sup>-3</sup>	261	214	<0.84
22	3.6	21°36'45"	40°56'30"	2.6	(0.158 ± 0.019)	(6.58 ± 0.52)	(1.29 ± 0.14) × 10 <sup>-3</sup>	(2.81 ± 0.32) × 10 <sup>-3</sup>	267	219	<0.84
23	8.6	21°36'19"	40°55'36"	12.3	(0.186 ± 0.017)	(6.41 ± 0.46)	(1.37 ± 0.15) × 10 <sup>-3</sup>	(3.35 ± 0.38) × 10 <sup>-3</sup>	207	167	2.22
24	13.6	21°35'47"	40°52'47"	33.3	(0.156 ± 0.014)	(3.13 ± 0.28)	(1.62 ± 0.18) × 10 <sup>-3</sup>	(1.33 ± 0.15) × 10 <sup>-3</sup>	52	49	11.3
25	18.6	21°35'15"	40°49'50"	34.6	(0.091 ± 0.013)	(1.368 ± 0.099)	(1.55 ± 0.17) × 10 <sup>-3</sup>	(1.30 ± 0.15) × 10 <sup>-3</sup>	41	43	11.8
26	25.6	21°34'36"	40°45'55"	34.8	(0.080 ± 0.010)	(2.15 ± 0.16)	(1.67 ± 0.19) × 10 <sup>-3</sup>	(1.31 ± 0.15) × 10 <sup>-3</sup>	47	43	11.7
27	32.6	21°33'58"	40°42'00"	35.4	(0.088 ± 0.009)	(1.073 ± 0.095)	(1.55 ± 0.17) × 10 <sup>-3</sup>	(9.0 ± 1.0) × 10 <sup>-4</sup>	41	42	11.7

In fresh waters, radium is intensely adsorbed to particles. On the other hand, in salty waters, radium appears mainly as a dissolved species. These differences in the behavior of radium are due to a change in the coefficient of adsorbed radium between freshwater and seawater (Moore and Oliveira, 2008). Existing sediments close to the coast and at depths reaching a few centimeters of the sediment bottom layer offer a continuous source of the short half-life radium isotopes (<sup>223</sup>Ra and <sup>224</sup>Ra). This is because thorium isotopes are strongly linked to sediment particles and radium is incorporated in salty water whenever sediment mixing occurs (Moore, 2000a,b). The long half-life radium isotopes (<sup>226</sup>Ra and <sup>228</sup>Ra) are also supplied by sediments, but in lower activities (Moore et al., 1995; Moore, 2000a,b). Groundwater is also a source of <sup>228</sup>Ra, <sup>226</sup>Ra <sup>223</sup>Ra and <sup>224</sup>Ra (Krest et al., 1999; Moore, 2000a,b; Moore and Krest, 2004). However, as most sediments present a higher <sup>232</sup>Th activity in relation to <sup>235</sup>U, the initial <sup>224</sup>Ra activity will be considerably higher than that of <sup>223</sup>Ra (Moore and Krest, 2004).

Distributions of barium have been intensively investigated in various estuaries and coastal waters (Li and Chan, 1979; Carroll et al., 1993; Moore, 1997; Moore and Shaw, 1998). Li and Chan (1979) first demonstrated that barium desorption from river-borne sediments effectively increases the flux to the ocean in the Hudson River estuary. Desorption of elements bound to particles presumably occurs owing to a decrease in their adsorption coefficients with increasing ionic strength (Nozaki et al., 2001).

**Table 3**  
Calculated Pearson correlation coefficients for the 1st sampling campaign.

	Si	Ba	Salinity	<sup>228</sup> Ra	<sup>226</sup> Ra	Distance
Si	1	.992 <sup>a</sup>	-.997 <sup>a</sup>	-.162	-.004	-.666 <sup>b</sup>
Ba	.992 <sup>a</sup>	1	-.989 <sup>a</sup>	-.264	-.178	-.693 <sup>a</sup>
Salinity	-.997 <sup>a</sup>	-.989 <sup>a</sup>	1	.254	.190	.648 <sup>a</sup>
<sup>228</sup> Ra	-.162	-.264	.254	1	.012	-.006
<sup>226</sup> Ra	-.004	-.178	.190	.012	1	.424 <sup>b</sup>
Distance	-.666 <sup>b</sup>	-.693 <sup>a</sup>	.648 <sup>a</sup>	-.006	.424 <sup>b</sup>	1

<sup>a</sup> The correlation is significant at 0.01 levels (2-tailed).

<sup>b</sup> The correlation is significant at 0.05 levels (2-tailed).

The behavior of barium in estuarine waters is dominated by release from particle phases in the low to moderate salinity ranges. This is very similar to the behavior of radium (Pettersen et al., 2008). Most of the release is attributed to ion exchange between major cations of seawater and barium bound to the riverine-suspended particle load. The removal processes include coprecipitation with iron (Fe) and manganese (Mn) phases, as well as uptake during phytoplankton blooms within the estuary (Nozaki et al., 2001; Coffey et al., 1997). Estuarine and salt marsh sediments can be an additional source of barium through remineralization from particulate phases. Another major source of barium to high salinity estuarine waters comes from the exchange of Ba-rich ground and pore waters with the tidal prism (Moore and Shaw, 2008).

The behavior of uranium in estuarine waters is frequently characterized as conservative mixing of the relatively enriched seawater end-member with low freshwater end-members. However, uranium displays non-conservative behavior in the upper estuary (low salinity) and in the high salt marsh. This is a result of binding to colloids, such as humic and fulvic acids and/or iron hydroxides. These reactions potentially reduce the net river flux of uranium to the ocean. Non-conservative behavior has also been observed in the lower, more saline estuary (Moore and Shaw, 2008).

In continental surface waters, uranium mainly comes from the presence of naturally occurring radioactive materials in the Earth's

**Table 4**  
Calculated Pearson correlation coefficients for the 2nd sampling campaign.

	Si	Ba	Salinity	<sup>228</sup> Ra	<sup>226</sup> Ra	Distance	U
Si	1	.928 <sup>a</sup>	-.962 <sup>a</sup>	.779 <sup>a</sup>	-.182	-.799 <sup>a</sup>	-.996 <sup>a</sup>
Ba	.928 <sup>a</sup>	1	-.964 <sup>a</sup>	.910 <sup>a</sup>	-.157	-.851 <sup>a</sup>	-.994 <sup>a</sup>
Salinity	-.962 <sup>a</sup>	-.964 <sup>a</sup>	1	-.834 <sup>a</sup>	.223	.847 <sup>a</sup>	.996 <sup>a</sup>
<sup>228</sup> Ra	.779 <sup>a</sup>	.910 <sup>a</sup>	-.834 <sup>a</sup>	1	.036	-.826 <sup>a</sup>	-.895 <sup>a</sup>
<sup>226</sup> Ra	-.182	-.157	.223	.036	1	-.032	.141
Distance	-.799 <sup>a</sup>	-.851 <sup>a</sup>	.847 <sup>a</sup>	-.826 <sup>a</sup>	-.032	1	.816 <sup>a</sup>
U	-.996 <sup>a</sup>	-.994 <sup>a</sup>	.996 <sup>a</sup>	-.895 <sup>a</sup>	.141	.816 <sup>a</sup>	1

<sup>a</sup> The correlation is significant at 0.01 levels (2-tailed).

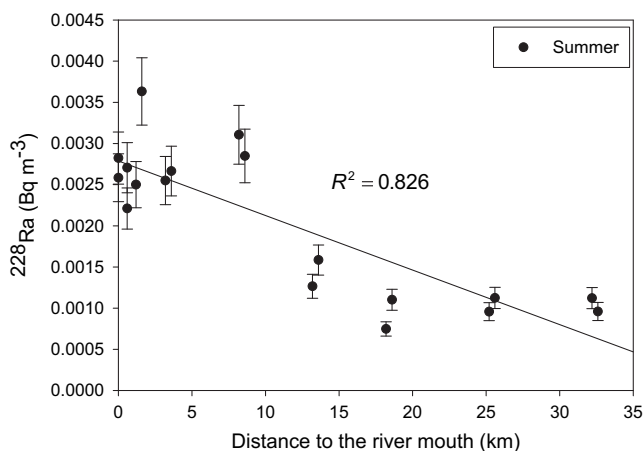


Fig. 2.  $^{228}\text{Ra}$  as a function of distance in relation to the coast, for surface water samples in March 2008.

crust. Its release is primarily controlled by weathering rates of the source rocks. Uranium solubility depends on its valence state: under reducing conditions  $\text{U}^{4+}$  is insoluble and under oxidizing conditions  $\text{U}^{6+}$  is soluble.

Most surface waters are oxidizing. Therefore,  $\text{U}^{6+}$  forms various soluble complexes with ions, such as bicarbonate. In estuaries, dissolved uranium ( $\text{U}^{\text{D}}$ ) behaves in a globally conservative manner and shows a linear relationship with salinity (Saari et al., 2008).

The main objective of the present study was to examine the existing water-mixing mechanisms in the Paraíba do Sul River estuarine region and to evaluate the extent of its waters by applying different natural tracers (i.e., salinity, silicon, barium, uranium and radium isotopes).

## 2. Study area and experimental

The Brazilian southeast region includes the states of Minas Gerais, Espírito Santo, Rio de Janeiro and São Paulo. The combined area of these states corresponds to nearly 9% of the Brazilian territory. However, 43% of population and 57% of the Brazilian gross domestic product (GDP) are concentrated in this region. This fact demonstrates the relevance of the southeast region for the Brazilian economy and for national development. Moreover, the southeast is the home of one of the most important rivers on the eastern Brazilian coast, the Paraíba do Sul River. The Paraíba do Sul River has a catchments area of approximately 55,400 km<sup>2</sup>, with 1500 km of extension. It crosses the states of Minas Gerais, São Paulo and Rio de Janeiro. The Paraíba do Sul estuary is located at a coastal plain

formed by the Paraíba do Sul River delta in the north of Rio de Janeiro State, near São João da Barra (21°36' S and 41°05' W) (Gonçalves and Carvalho, 2006). Its discharge flux can reach up to 4400 m<sup>3</sup> s<sup>-1</sup> during the rainy period (summer), decreasing to 180 m<sup>3</sup> s<sup>-1</sup> in the dry season (winter). As a result, the Paraíba do Sul River is the main source of water for more than 11,000,000 people in the city of Rio de Janeiro alone (Carvalho et al., 2002).

### 2.1. Sampling

The first sampling campaign at the Paraíba do Sul River estuary (PSR) was conducted from August 7–9, 2007, during the winter season. At this time of year there is a predominance of dry weather and the river presents a low water outflow discharge into the ocean (330 m<sup>3</sup> s<sup>-1</sup>). This campaign was carried out in three transects, as indicated in Fig. 1, with the third transect following the same sampling points as the first one.

The second sampling campaign was conducted from March 4–6, 2008, during the summer season. At this time of year there is a predominance of rainy weather and the river presents a high water outflow discharge into the ocean (780 m<sup>3</sup> s<sup>-1</sup>). This campaign was carried out in three transects, as indicated in Fig. 1.

### 2.2. Determination of radium isotopes

At a sampling depth of one meter, large volume (100–200 L) seawater samples were collected in plastic tanks and the sample volume was recorded. Water was pumped at a rate of 1 L min<sup>-1</sup> through two sequential columns, one containing pure acrylic fiber and the other containing MnO<sub>2</sub>-coated acrylic fiber. This was carried out to remove particulates and to quantitatively adsorb radium (Moore 1976). Filtered sub-samples (50 mL) were taken for further determination of salinity, barium, uranium and silicon content. These were kept at 4 °C until analyses could be performed.

Each MnO<sub>2</sub>-fiber sample containing radium was partially dried (approximately 50% water) and connected to a RaDeCC™ system (Scientific Instruments). Helium was circulated through the manganese fiber to remove <sup>219</sup>Rn and <sup>220</sup>Rn generated by the decay of <sup>223</sup>Ra and <sup>224</sup>Ra. Both isotopes passed through a scintillation cell, where alpha particles emitted from the radon and its daughter products were detected by a photomultiplier tube (PMT) coupled to the cell. Pulses generated in the PMT were then directed to a delayed coincidence system, as proposed by Giffin et al. (1963) and adapted for radium measurements by Moore and Arnold (1996). The delayed coincidence counting system utilizes the difference between the isotope decay constants of short half-life polonium isotopes, the daughter of <sup>219</sup>Rn and <sup>220</sup>Rn, to identify particles alpha of the decay

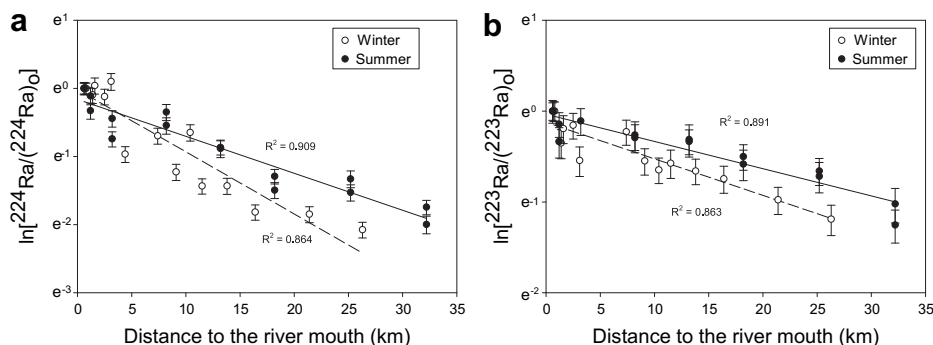


Fig. 3.  $^{223}\text{Ra}$  and  $^{224}\text{Ra}$  as a logarithmic function of the distance to the river mouth, for surface water samples collected in August 2007(a) and March 2008(b).

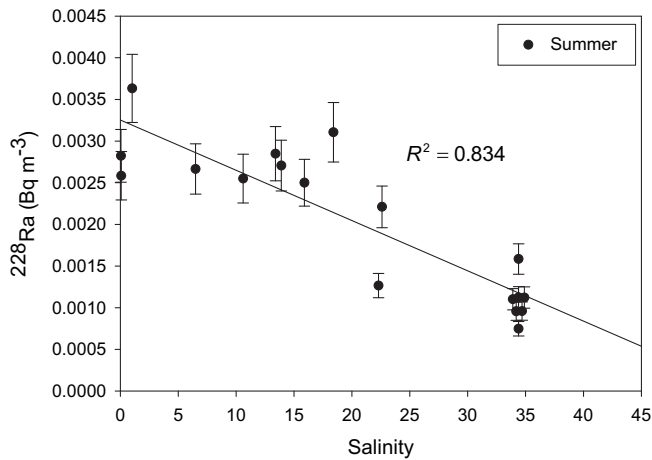


Fig. 4.  $^{228}\text{Ra}$  as a function of salinity in relation to the coast, for surface water samples taken in March 2008.

of  $^{219}\text{Rn}$  and  $^{220}\text{Rn}$ . Thus, this enables determination of the activities of the retained  $^{223}\text{Ra}$  and  $^{224}\text{Ra}$  in the manganese fiber.

The samples were initially measured shortly after sampling, with a second measurement being carried out after two weeks and a third counting after one month. The first measurement was used to calculate the  $^{224}\text{Ra}$  concentration, the second measurement to calculate the  $^{223}\text{Ra}$  concentration and the last measurement to calculate  $^{228}\text{Th}$ . The activity of  $^{228}\text{Th}$  was needed for necessary corrections of the results regarding supported  $^{224}\text{Ra}$ .

After these determinations, the manganese fibers were leached with concentrated HCl and hydroxylamine hydrochloride, so that the long half-life radium isotopes could be quantitatively removed. Radium was co-precipitated with  $\text{BaSO}_4$  and the alpha count of  $^{226}\text{Ra}$  was measured using a low-level proportional counter (Prof. Berthold, model LB 770). This was performed after approximately 21 days of precipitation, which was necessary to ensure that the radioactive equilibrium  $^{226}\text{Ra}$ – $^{222}\text{Rn}$  had been reached. This was also true for  $^{224}\text{Ra}$  and  $^{223}\text{Ra}$  decay, as described by Godoy et al. (1994).  $^{228}\text{Ra}$  was determined by beta counting of the same precipitate. The  $\text{BaSO}_4$  precipitate was covered with a filter paper having equal diameter to the container, blinding the detector to  $^{226}\text{Ra}$  alpha particles, and beta particles from the isotope of interest were counted. The reported uncertainties are the combined standard uncertainties calculated according to the Eurachem/Citac Guide CG-4 (2000). Involved equations are similar to those developed by Garcia-Solsona et al. (2008), but also include the uncertainty related to calibration standards for the counting systems.

### 2.3. Silicon, barium, uranium and salinity

Concentrations of silicon and barium in seawater samples were determined by Inductively Coupled Plasma-Optical Emission Spectroscopy (ICP-OES; Perkin Elmer, model: Optima 4300 DV). Direct analysis was used without dilution and scandium was applied as internal standard.

During the second sampling campaign, the  $^{238}\text{U}$  concentration in seawater samples was determined by Inductively Coupled Plasma Mass Spectrometry (ICP-MS; Varian, model: 820 MS). Analysis was performed after dilution by 1:100 and thallium (Tl) was applied as internal standard.

The salinity of samples was measured with a pH/Conductivity Pocket Meter (WTW, model: pH/Cond 340i), which was calibrated with a solution of KCl ( $35 \text{ g kg}^{-1}$ ). All salinity measurements were performed at  $25^\circ\text{C}$ .

## 3. Results and discussion

Results obtained during the first sampling campaign (dry season) are shown in Table 1 and those obtained during the second campaign (rainy season) are shown in Table 2. In the PSR estuarine region, the balance between advection and diffusion changes with a relatively high frequency. This is particularly true during the winter season, which is when cold fronts arrive. Although the weather and sea conditions were quite stable during both sampling campaigns, it is not possible to ensure the absence of an advective component. It is also difficult to pinpoint the reason for the non-linear correlation between  $^{228}\text{Ra}$  concentration and distance to the river mouth, which was observed during the winter campaign, as a consequence of advection or low river discharge flow. On the other hand, it is possible to affirm that a diffusive mechanism was more frequent during the summer than during the winter. Also, for the same period, a higher flow discharge favored the application of radium isotopes as a tool to study water mixing in the estuarine region. The observed results confirm these conclusions. Higher Pearson correlation coefficients, relating the distance of sampling points to the PSR estuary and the determined parameters, were found during the summer versus the winter season (Tables 3 and 4). In particular, statistically significant correlations of  $^{228}\text{Ra}$ , barium, salinity, silica and uranium with distance and salinity were observed during this period of higher river discharge flow. Although the existence of advective processes could not be dismissed, these linear correlations with distance (see Fig. 2 for  $^{228}\text{Ra}$ ), which associate the logarithmic behavior of both  $^{223}\text{Ra}$  and  $^{224}\text{Ra}$  with the distance to the river mouth (Fig. 3b), demonstrate that diffusion is an important dispersion mechanism for deriving conservative elements from the Paraíba do Sul River.

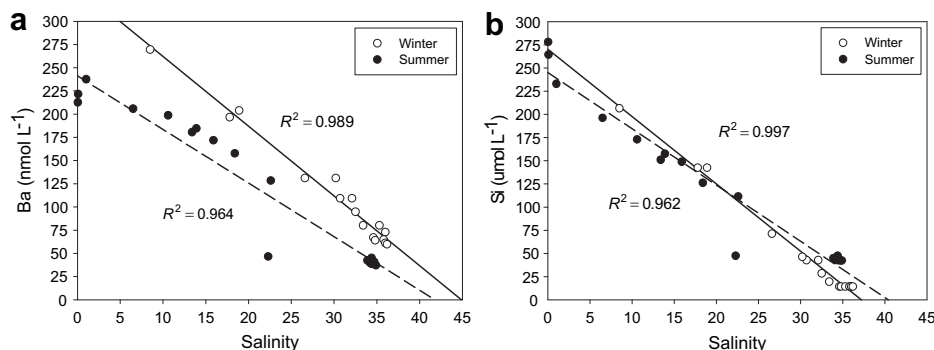


Fig. 5. Ba (a) and Si (b) concentration as a function of the salinity, for surface water samples collected in August 2007 and March 2008.

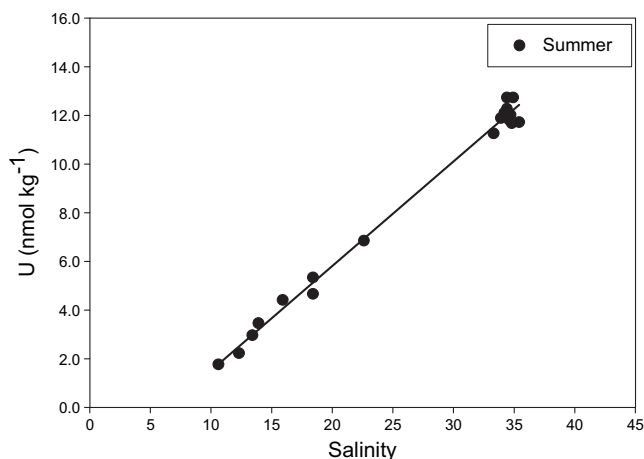


Fig. 6. U concentration as a function of salinity, for surface water samples collected in March 2008.

Both short-lived radium isotopes ( $^{223}\text{Ra}$  and  $^{224}\text{Ra}$ ) followed an exponential variation in relation to distance for both sampling campaigns (Fig. 3a and b). Using the slope of the correlation graphs, it was possible to obtain the diffusion coefficient ( $K_h$ ), as proposed by Moore (2000a,b), and the obtained results were:  $23 \text{ km}^2 \text{ d}^{-1}$  ( $R^2 = 0.891$ ) for  $^{224}\text{Ra}$  and  $38 \text{ km}^2 \text{ d}^{-1}$  ( $R^2 = 0.863$ ) for  $^{223}\text{Ra}$ , for the first sampling campaign, and  $65 \text{ km}^2 \text{ d}^{-1}$  ( $R^2 = 0.864$ ) for  $^{223}\text{Ra}$  and  $68 \text{ km}^2 \text{ d}^{-1}$  ( $R^2 = 0.909$ ) for  $^{224}\text{Ra}$ , for the second sampling campaign. Owing to the higher river outflow during the rainy season, a closer coincidence was observed between the  $^{223}\text{Ra}$  and  $^{224}\text{Ra}$   $K_h$  results compared to those obtained during the dry season. This closer coincidence also provides additional evidence for a diffusive process, in contrast to results obtained for the winter campaign. Comparison of the second sampling in March, when the Paraíba do Sul River had a high outflow, to the first sampling in August, when the river had a low outflow, revealed a substantial increase in the diffusion coefficient on the order of 3.

The northern area of the state of Rio de Janeiro is known for the presence of monazite at its beaches. There is also a monazite extraction plant in the nearby city of San Francisco de Itabapoana. As monazite is a source of thorium (Th), the observed concentrations of  $^{228}\text{Ra}$  were greater than those of  $^{226}\text{Ra}$ . This is in contrast to the values observed by Moore and Shaw (2008) for several US estuaries. On the other hand, the values obtained in the present work are similar to those found in the region of Ubatuba and Ilha Grande Bay (Godoy et al., 2006; Burnett et al., 2008; Moore and Oliveira, 2008). Fig. 4 shows the dependence of  $^{228}\text{Ra}$  on salinity for the summer campaign (rainy season). The higher concentrations observed at low salinity, just beyond the river mouth, can be

indicative of adsorbed radium release from particulates due to increased salinity (Krest et al., 1999). Positive deviations observed at salinities around 15 could be from the influence of tide height, as higher salinities were observed closer to the river discharge mouth during high tide events compared to low tide events.

Barium showed conservative salinity behavior during both sampling campaigns (Fig. 5). Owing to the low river discharge during the dry season, it was not possible to determine the river end-member. This is because the lowest measured salinity was 8.5, indicating that mixing with seawater was already occurring (Table 1). However, during the rainy season, a salinity as low as 0.1 was measured at the river mouth, which indicates a low mixture degree with seawater. Based on this sampling point, a barium river end-member of about  $220 \text{ nmol L}^{-1}$  was estimated (Table 2). By comparing both sampling campaigns, it was possible to verify a seasonal variation in low salinity values with river water end-member high concentrations during the dry season, as also reported by Nozaki et al. (2001) for the Chao Phraya river estuary in Thailand. Based on observed results for the sampling point at 32 km from the shoreline (Table 2), the seawater barium end-member was around  $40 \text{ nmol L}^{-1}$ , which is similar to values reported by Shaw et al. (1998;  $38 \text{ nmol L}^{-1}$  for surface Atlantic waters) and Vegería et al. (2002);  $40\text{--}50 \text{ nmol L}^{-1}$  for seawater samples 60 km from the same coast studied in the present work. As verified by other authors (Nozaki et al., 2001; Moore and Shaw, 2008), an increase in the barium concentration was observed in the low salinity mixing zone ( $S \sim 5$ ) and then a linear decrease was observed for higher salinity waters. Similarly, as verified for  $^{228}\text{Ra}$  in the summer period (Fig. 4), the positive deviation observed at higher salinity ( $\sim 15$ ) could be from the influence of tide height, as higher salinities were observed close to the river discharge mouth during high tide events.

Silicon shows a quite similar pattern (Fig. 5b), with its concentration mainly controlled by seawater dilution, as shown by a negative linear relationship to the salinity. However, silicon has its maximum concentration at the lowest salinity value, in contrast with barium. Zhang (1996) has shown that, in large Chinese estuaries, silicon can present either conservative or non-conservative behavior, with the riverine silicon end-member between  $110\text{--}170 \text{ nmol L}^{-1}$ , reaching levels up to  $300 \text{ nmol L}^{-1}$  for the Huanghe River. Based on the results shown in Fig. 3b, the PSR silicon end-member can be as high as the value reported by Zhang (1996). On the hand, no seasonal effect was observed for silicon, as verified for barium and as reported by Zhang (1996). The anomalous value observed at  $S \sim 20$  (Fig. 5a and b) is verified for both barium and silicon, indicating the inflow of higher salinity waters. This occurred during the second transect from the second sampling campaign, when an attempt to follow the river plume was performed.

During the second sampling campaign, it was still possible to observe a strong correlation between the results obtained for

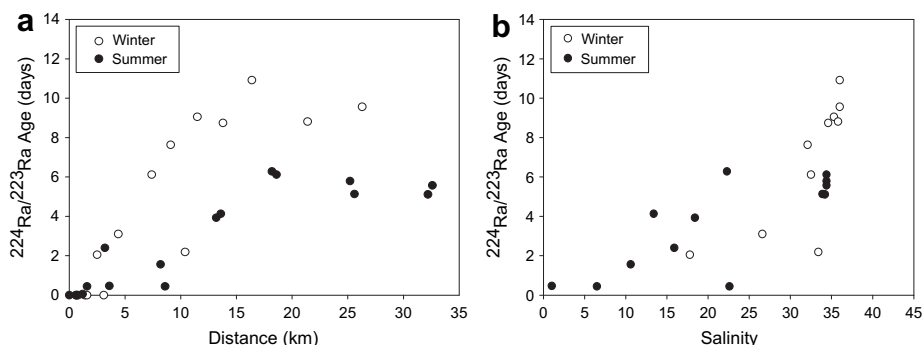


Fig. 7.  $(^{224}\text{Ra}/^{223}\text{Ra})_{\text{age}}$  as a function of the distance in relation to the river mouth (a) and as a function of the salinity for surface water samples (b) in August 2007 and March 2008.

uranium and salinity, as shown in Fig. 6. The conservative behavior of uranium indicates that was probably present as a U(VI) carbonate complex. The ocean uranium end-member was  $13 \text{ nmol L}^{-1}$ , which is close to the value of  $13.6 \text{ nmol L}^{-1}$  for  $S = 35$  reported by McKee (2008).

Assuming that the  $^{224}\text{Ra}/^{223}\text{Ra}$  activity ratio is constant near the shore and only diminishes as surface water is isolated from the water sources (Moore, 2000b), it was possible to calculate the residence time of the Paraíba do Sul River plume in the open ocean direction. Despite the weakness of such an assumption for an estuarine region, coherent results were obtained for calculated ages when comparing dry and rainy seasons. During the dry season, the time necessary for the deriving waters of the Paraíba do Sul River to reach a distance of about 16 km in relation to the coast was approximately 10 days (Fig. 7a). On the other hand, in the rainy season (summer) the same process took approximately 6 days (Fig. 7a). This results in velocities of 1.6 and  $2.6 \text{ km d}^{-1}$  during the dry and rainy periods, respectively. Fig. 7b shows that, during the low river water discharge period, the riverine water took about 10 days to reach the open ocean waters ( $S \sim 35$ ) and, during the rainy period, the river waters reaching this region were much younger (6 days).

#### 4. Conclusion

Based on the results obtained during the two sampling campaigns (for two seasons, including winter and summer), it was possible to conclude that the multitracers used [i.e., salinity, silicon, barium, uranium and radium isotopes ( $^{223}\text{Ra}$ ,  $^{224}\text{Ra}$ ,  $^{226}\text{Ra}$  and  $^{228}\text{Ra}$ )] presented satisfactory results for the delimitation of the plume reach, residence time, and water-mixing processes in the Paraíba do Sul River estuary. A strong correlation was observed between the tracers and the distance to the coast. During the low river water discharge period, the riverine water took about 10 days to reach the open ocean waters ( $S \sim 35$ ). Whereas, during the rainy period, the river waters reaching this region were much younger.

#### Acknowledgements

The authors thank UENF (Universidade Estadual do Norte Fluminense) for support during field work, the IRD/CNEN for logistical support needed to accomplish the analyses, Maurício Dupim and André Vechi (Chemistry Department, PUC-Rio) for silicon and barium determinations by ICP-OES, Prof. Dr. Ricardo Aucélio for linguistic advice, and FAPERJ for financial support during the course of this study. This project was also partially supported by the CNPq, through the INCT “Transferência de matéria continente-oceano”, process number 573.601/2008-9.

#### References

Burnett, W.C., Peterson, R., Moore, W.S., Oliveira, J.de, 2008. Radon and radium isotopes as tracers of submarine groundwater discharge e results from the Ubatuba, Brazil SGD assessment intercomparison. *Estuarine, Coastal and Shelf Science* 76, 501–511.

Carroll, J., Falkner, K.K., Brown, E.T., Moore, W.S., 1993. The role of the Ganges Brahmaputra mixing zone in supplying barium and  $^{226}\text{Ra}$  to the Bay of Bengal. *Geochimica et Cosmochimica Acta* 57, 2981–2990.

Carvalho, C.E.V., Salomão, M.S.M.B., Molisani, M.M., Rezende, C.E., Lacerda, L.D., 2002. Contribution of a medium-sized tropical river to the particulate heavy-metal load for the South Atlantic Ocean. *The Science of the Total Environment* 284, 85–93.

Charette, M.A., Moore, W.S., Burnett, W.C., 2008. Uranium and thorium series nuclides as tracers of submarine groundwater discharge. In: Krishnaswami, S.,

Cochran, J.K. (Eds.), U–Th Series Nuclides in Aquatic Systems. *Radioactivity in the Environment Series*, vol. 13. Elsevier, Oxford, UK, pp. 155–192.

Coffey, M., Dehairs, F., Collette, O., Luther, G., Church, T., Jickells, T., 1997. The behavior of dissolved barium in estuaries. *Estuarine, Coastal and Shelf Science* 45, 113–121.

Eurachem/Citac, 2000. Quantifying Uncertainty in Analytical Measurement, Report CG-4, second ed.

García-Solsona, E., García-Orellana, J., Masqué, P., Dulaiova, H., 2008. Uncertainties associated with  $^{223}\text{Ra}$  and  $^{224}\text{Ra}$  measurements in water via a delayed coincidence counter (RaDeCC). *Marine Chemistry* 109, 198–219.

Giffin, C., Kaufman, A., Broecker, W., 1963. Delayed coincidence counter for the assay of actinon and thoron. *Journal of Geophysical Research* 68 (6), 1749–1757.

Godoy, J.M., Lauria, D.C., Godoy, M.L.D.P., Cunha, R.P., 1994. Development of a sequential method for the determination of  $^{238}\text{U}$ ,  $^{234}\text{U}$ ,  $^{232}\text{Th}$ ,  $^{230}\text{Th}$ ,  $^{228}\text{Th}$ ,  $^{226}\text{Ra}$ , and  $^{210}\text{Pb}$  in environmental samples. *Journal of Radioanalytical and Nuclear Chemistry* 182 (1), 165–169.

Godoy, J.M., Carvalho, Z.L., Fernandes, F.C., Danelon, O.M., Godoy, M.L.D.P., Ferreira, A.C.M., Roldão, L.A., 2006.  $^{228}\text{Ra}$  and  $^{226}\text{Ra}$  in coastal seawater samples from the Ubatuba region – Brazilian southeastern coastal region. *Journal of the Brazilian Chemical Society* 17 (4), 730–736.

Gonçalves, G.M., Carvalho, C.E.V., 2006. Particulate heavy metal dynamics in a tropical estuary under distinct river discharge and tidal regimes, South-eastern, Brazil. *Journal of Coastal Research Special Issue* 39 (2), 1032–1035.

Krest, J.M., Moore, W.S., Rama, 1999.  $^{226}\text{Ra}$  and  $^{228}\text{Ra}$  in the mixing zones of Mississippi and Atchafalaya Rivers: indicators of groundwater input. *Marine Chemistry* 64, 129–152.

Lee, J.S., Kim, K.H., Moon, D.S., 2005. Radium isotopes in the Ulsan Bay. *Journal of Environmental Radioactivity* 82, 129–141.

Levy, D.M., Moore, W.S., 1985.  $^{224}\text{Ra}$  in continental shelf waters. *Earth and Planetary Science Letters* 73, 226–230.

Li, Y.L., Chan, L.-H., 1979. Desorption of Ba and  $^{226}\text{Ra}$  from river-borne sediments in the Hudson estuary. *Earth and Planetary Science Letters* 43, 343–350.

McKee, B.A., 2008. U- and Th-series nuclides in estuarine environments. In: Krishnaswami, S., Cochran, J.K. (Eds.), U–Th Series Nuclides in Aquatic Systems. *Radioactivity in the Environment Series*, vol. 13. Elsevier, Oxford, UK, pp. 193–226.

Moore, W.S., 1976. Sampling radium-228 in the deep ocean. *Deep-Sea Research* 23, 647–651.

Moore, W.S., Astwood, H., Lindstrom, C., 1995. Radium isotopes in coastal waters on the Amazon shelf. *Geochimica et Cosmochimica Acta* 59 (20), 4285–4298.

Moore, W.S., 1997. High fluxes of radium and barium from the mouth of the Ganges-Brahmaputra River during low river discharge suggest a large groundwater source. *Earth and Planetary Science Letters* 150, 141–150.

Moore, W.S., 2000a. Determining coastal mixing rates using radium isotopes. *Continental Shelf Research* 20, 1993–2007.

Moore, W.S., 2000b. Ages of continental shelf waters determined by  $^{223}\text{Ra}$  and  $^{224}\text{Ra}$ . *Journal of Geophysical Research* 20, 1995–2007.

Moore, W.S., Arnold, R., 1996. Measurement of  $^{223}\text{Ra}$  and  $^{224}\text{Ra}$  in coastal waters using a delayed coincidence counter. *Journal of Geophysical Research* 101 (C1), 1321–1329.

Moore, W.S., Krest, J., 2004. Distribution of Ra-223 and Ra-224 in the plumes of the Mississippi and Atchafalaya Rivers and the Gulf of Mexico. *Marine Chemistry* 86, 105–119.

Moore, W.S., Oliveira, J., 2008. Determination of residence time and mixing processes of the Ubatuba, Brazil, inner shelf waters using natural Ra isotopes. *Estuarine, Coastal and Shelf Science* 76, 512–521.

Moore, W.S., Shaw, T.J., 1998. Chemical signals from submarine fluid advection onto the continental shelf. *Journal of Geophysical Research* 103, 21543–21552.

Moore, W.S., Shaw, T.J., 2008. Fluxes and behavior of radium isotopes, barium, and uranium in seven Southeastern US rivers and estuaries. *Marine Chemistry* 108, 236–254.

Nozaki, Y., Yamamoto, Y., Manaka, T., Amakawa, H., Snidvongs, A., 2001. Dissolved barium and radium isotopes in the Chao Phraya River estuarine mixing zone in Thailand. *Continental Shelf Research* 21, 1435–1448.

Petterson, R.N., Burnett, W.C., Taniguchi, M., Chen, J., Santos, I.R., Misra, S., 2008. Determination of transport rates in the Yellow River–Bohai Sea mixing zone via natural geochemical tracers. *Continental Shelf Research* 28, 2700–2707.

Saari, H.-K., Schmidt, S., Huguot, S., Lanoux, A., 2008. Spatiotemporal variation of dissolved  $^{238}\text{U}$  in the Gironde fluvial-estuarine system (France). *Journal of Environmental Radioactivity* 99, 426–435.

Shaw, T.J., Moore, W.S., Kloeper, J., Sockaski, M.A., 1998. The flux of barium to the coastal waters of the southeastern United States: the importance of submarine groundwater discharge. *Geochimica et Cosmochimica Acta* 62, 3047–3052.

Veguería, S.F.J., Godoy, J.M., Miekeley, N., 2002. Environmental impact in sediments and seawater due to discharges of Ba,  $^{226}\text{Ra}$ ,  $^{228}\text{Ra}$ , V, Ni and Pb by produced water from the Bacia de Campos oil field offshore platforms. *Environmental Forensics* 3, 115–123.

Zhang, J., 1996. Nutrients elements in large chinese estuaries. *Continental Shelf Research* 16, 1023–1045.